

# Addressing $H_0$ tension by means of VCDM

Antonio De Felice,<sup>1,\*</sup> Shinji Mukohyama,<sup>1,2,†</sup> and Masroor C. Pookkillath<sup>1,‡</sup>

<sup>1</sup>*Center for Gravitational Physics, Yukawa Institute for Theoretical Physics, Kyoto University, 606-8502, Kyoto, Japan*

<sup>2</sup>*Kavli Institute for the Physics and Mathematics of the Universe (WPI),  
The University of Tokyo, Kashiwa, Chiba 277-8583, Japan*

In this letter we propose a reduction of the  $H_0$  tension puzzle by means of a theory of minimally modified gravity which is dubbed VCDM. After confronting the theory with the data, a transition in the expansion history of the universe in the low-redshift  $z \simeq 0.3$  is found. From the bestfit values the total fitness parameter is improved by  $\Delta\chi^2 = 33.41$ , for the data set considered. We then infer the local Hubble expansion rate today within this theory by means of low redshift Pantheon data. The resulting local Hubble expansion rate today is  $H_0^{\text{loc}} = 73.69 \pm 1.4$ . Hence the tension is reduced within the VCDM theory.

The value of today's rate of expansion of the universe,  $H_0$ , has been measured, as a direct measurement, from low-redshift observations, namely, SH0ES [1], H0LiCOW [2], Megamaser Project [3] (MCP) and Carnegie-Chicago Hubble Program (CCHP) Collaboration [4]. Among these observations SH0ES in particular has achieved a remarkable precision providing  $H_0 = 74.03 \pm 1.42$  (in units of  $\text{km s}^{-1} \text{Mpc}^{-1}$ ). On the other hand, on assuming some theoretical model,  $H_0$  can also be deduced from the measurement of temperature power spectra in the Cosmic Microwave Background (CMB) which is produced at the recombination time. The recent Planck Legacy 2018 release gives  $H_0 = 67.04 \pm 0.5$ , assuming the standard flat- $\Lambda$ CDM model (non-flat versions are known to be strongly disfavored by other data, e.g. Baryon Acoustic Oscillations (BAO)) [5]. Hence, the tension between this theoretical model and experimental results adds up to more than  $4\sigma$ 's [6, 7].

However, the flat- $\Lambda$ CDM could be representing only a first approximation to another, improved model of our universe. The VCDM theory, described in the following, was originally introduced for the purpose of seeking minimal theoretical deviations from the standard model of gravity and cosmology, i.e. General Relativity (GR) and  $\Lambda$ CDM, as it does not introduce any new propagating physical degrees of freedom in the gravity sector, but on the other hand, one can have, as we will show in the following, a non-trivial and interesting phenomenology.

In the VCDM theory [8], the cosmological constant  $\Lambda$  in the standard  $\Lambda$ CDM is promoted to a function  $V(\phi)$  of a non-dynamical, auxiliary field  $\phi$ . This theory of modified gravity breaks four dimensional diffeomorphism invariance at cosmological scales but keeps the three dimensional spatial diffeomorphism invariance. On doing so, the theory modifies gravity at cosmological scales while it only possess two gravitational degrees of freedom as in GR. In general this allows a spectrum of possibilities typically much larger than the case of a scalar-tensor theory. For the latter, the extra scalar degree of freedom leads to strong constraints not only on solar system scales (for which one needs the scalar to be very massive or to be shielded by some non-trivial dynamical mechanisms,

e.g. chameleon or Vainshtein), but also on cosmological scales (for which one needs to constrain the background dynamics as to avoid ghost and gradient instabilities).

The equations of motion for the VCDM theory on a homogeneous and isotropic background can be written as

$$V = \frac{1}{3}\phi^2 - \frac{\rho}{M_{\text{Pl}}^2}, \quad \frac{d\phi}{d\mathcal{N}} = \frac{3}{2} \frac{\rho + P}{M_{\text{Pl}}^2 H}, \quad \frac{d\rho_i}{d\mathcal{N}} - 3(\rho_i + P_i) = 0, \quad (1)$$

where  $\mathcal{N} = \ln(a/a_0)$  ( $a$  being the scale factor and  $a_0$  being its present value),  $H = \dot{a}/a^2$  is the Hubble expansion rate (a dot denotes differentiation with respect to the conformal time),  $\rho = \sum_i \rho_i$  and  $P = \sum_i P_i$  (the sum is over the standard matter species). Unless  $\rho + P = 0$ , the following equation follows from the above equations:  $\phi = \frac{3}{2}V\phi - 3H$ . When  $V$  is a linear function of  $\phi$ , as in  $V = \lambda_1 \phi + \lambda_0$ , then the equations of motion (1) reduce to

$$3H^2 = \frac{\rho}{M_{\text{Pl}}^2} + \Lambda, \quad H \frac{dH}{d\mathcal{N}} = -\frac{\rho + P}{2M_{\text{Pl}}^2}, \quad \frac{d\rho_i}{d\mathcal{N}} - 3(\rho_i + P_i) = 0, \quad (2)$$

where  $\Lambda \equiv \lambda_0 + 3\lambda_1^2/4 = \text{const.}$  These are nothing but the equations of motion in the standard  $\Lambda$ CDM model. Moreover, for this choice of  $V(\phi)$  the theory reduces to GR with a cosmological constant not only for the homogeneous and isotropic background but also for perturbations at any order. Hence, the VCDM theory extends the  $\Lambda$ CDM model by replacing the constant  $\Lambda$  with a free function  $V(\phi)$ . Yet, the VCDM theory does not introduce extra degrees of freedom in the sense that the number of independent initial conditions is the same as  $\Lambda$ CDM. The “V” of VCDM therefore stands for the free function  $V(\phi)$  introduced in this theory.

In the following we want to be able to use the free function  $V(\phi)$  in order to give any wanted background evolution for  $H$  which can be given as  $H = H(\mathcal{N})$ . From the 2nd of (1), having given  $H$  as a function of  $\mathcal{N}$ , then one obtains

$$\phi(\mathcal{N}) = \phi_0 + \int_{\mathcal{N}_0}^{\mathcal{N}} \frac{3}{2} \frac{\rho(\mathcal{N}') + P(\mathcal{N}')}{M_{\text{Pl}}^2 H(\mathcal{N}')} d\mathcal{N}', \quad (3)$$

where  $\phi_0 = \phi(\mathcal{N}_0)$ . Assuming that  $\rho + P > 0$ , and  $H > 0$ , the right hand side of (3) is an increasing function of  $\mathcal{N}$  and thus the function  $\phi(\mathcal{N})$  has a unique inverse function,  $\mathcal{N} = \mathcal{N}(\phi)$ . Obviously,  $\mathcal{N}$  is an increasing function of  $\phi$ . By combining this with the 1st of (1), one obtains

$$V(\phi) = \frac{1}{3}\phi^2 - \frac{\rho(\mathcal{N}(\phi))}{M_{\text{Pl}}^2}. \quad (4)$$

Therefore we have obtained a simple and powerful reconstruction mechanism for  $V$  for a given and wanted evolution of  $H$ <sup>1</sup>. Once  $V(\phi)$  is specified in this way, we know how to evolve not only the homogeneous and isotropic background but also perturbations around it.

Having shown the reconstruction of the potential  $V$  for a given evolution of  $H$ , we can search for a profile for  $H(z)$  that can potentially reduce the  $H_0$  tension. We introduce two choices of  $H(z)$  to address current cosmo-

logical tensions: one in the flat- $\Lambda$ CDM and the other in the VCDM. The former is  $H_\Lambda^2 \equiv H_{\Lambda 0}^2 [\tilde{\Omega}_\Lambda + \tilde{\Omega}_{m0}(1+z)^3 + \tilde{\Omega}_{r0}(1+z)^4]$ , where  $\tilde{\Omega}_\Lambda \equiv 1 - \tilde{\Omega}_{m0} - \tilde{\Omega}_{r0}$ , and the latter is

$$H^2 = H_\Lambda^2 + A_1 H_0^2 \left[ 1 - \tanh \left( \frac{z - A_2}{A_3} \right) \right], \quad (5)$$

with the idea that  $0 < A_2 < 2$ . In this case we have at early times, for  $z \gg |A_2|$ , that the system will tend to be the standard flat- $\Lambda$ CDM evolution, i.e.  $H^2 \approx H_\Lambda^2$ . Today, i.e. for  $z = 0$ , we have  $H_0^2 = H_\Lambda^2 + A_1 H_0^2 \left[ 1 + \tanh \left( \frac{A_2}{A_3} \right) \right]$ , which can be solved today for  $A_1$ , to give  $A_1 = (1 - H_{\Lambda 0}^2/H_0^2) [\tanh(A_2/A_3) + 1]^{-1}$ .

Let us further consider the following parameter redefinitions  $\tilde{\Omega}_{m0} = \Omega_{m0} H_0^2/H_{\Lambda 0}^2$ ,  $\tilde{\Omega}_{r0} = \Omega_{r0} H_0^2/H_{\Lambda 0}^2$ , and  $\beta_H = H_{\Lambda 0}/H_0$ , then we find

$$\frac{H^2}{H_0^2} = \Omega_{m0}(1+z)^3 + \Omega_{r0}(1+z)^4 + (1 - \beta_H^2) \frac{1 + \tanh \left( \frac{A_2 - z}{A_3} \right)}{1 + \tanh \left( \frac{A_2}{A_3} \right)} + \beta_H^2 \left( 1 - \frac{\Omega_{m0}}{\beta_H^2} - \frac{\Omega_{r0}}{\beta_H^2} \right). \quad (6)$$

So in total we have six background parameters (three more than  $\Lambda$ CDM). However, we can reduce them to five (two more than  $\Lambda$ CDM) by fixing  $A_3$  as we expect to have a large degeneracy (after assuming  $A_2 = \mathcal{O}(1)$ ). According to Akaike Information Criterion (AIC), we can accept the model if we can have an improvement of  $\chi^2$  larger than four in comparison with  $\Lambda$ CDM [9]. In fact, we will show later on that the  $\chi^2$  has improved remarkably by 33.41 with respect to  $\Lambda$ CDM. In particular, we will fix, later on,  $A_3$  to the value of  $10^{-3}$ .

Two things need to be noticed. First, having given the expression for  $H = H(z)$ , one can automatically deduce all the needed background expressions as well as all evolution equations for perturbations. Second, the fact we have a minimally modified gravity (VCDM)-component does not mean we are adding a physical dark-component degree of freedom. In fact, for this theory, there is no additional physical degree of freedom, beside the tensorial gravitational waves and the standard ones related to the presence of matter fields [8].

After having introduced the behavior of the VCDM

model on a homogeneous and isotropic background, we will test it against several cosmological data to see how well it can address the  $H_0$  tension. Here we use Planck Legacy 2018 data with `planck_highl_TTEEE`, `planck_lowl_EE`, and `planck_lowl_TT` [10], baryon acoustic oscillation (BAO) from 6dF Galaxy Survey [11] and the Sloan Digital Sky Survey [12, 13], and Pantheon data set comprised of 1048 type Ia supernovae [14]. We do not use the SH0ES consisting of a single data point [1]  $H_0 = 74.03 \pm 1.42$ . Instead, we infer the local value of Hubble expansion today  $H_0^{\text{loc}}$  using the Pantheon data and employing the analysis technique explained in [15, 16]. Here we have not included the Planck lensing data since it was reported that the lensing anomaly is present in the Planck legacy release [17, 18].

Both the background and linear perturbation equations of motion are implemented in the Boltzmann code CLASS [19], with covariantly corrected baryon equations of motion [20].

For a matter action at second order up to shear for a fluid we proceed here by first writing the Schutz-Sorkin Lagrangian (SSL) for a single fluid [20], as follows

<sup>1</sup> The potential  $V(\phi)$  is not unique. Even for the same choice of  $H(z)$ , the shape of the potential  $V(\phi)$  depends on the initial value of  $\phi$ , which can be chosen arbitrarily. Changing the initial value of  $\phi$  changes the potential  $V$  by a constant and a term linear in  $\phi$ . In any case, the potential does not enter both at the

level of the background and linear perturbation theory which are affected only by  $H(z)$  and its derivatives. Furthermore, VCDM theory reduces to GR whenever  $V_{,\phi\phi} = 0$ . See e.g. eq. (5.11) of [8], which shows  $w_\phi = -1$  whenever  $V_{,\phi\phi} = 0$

$$S_{\text{SSL}} = - \int d^4x \sqrt{-g} [\rho(n, s) + J^\mu (\partial_\mu \ell + \theta \partial_\mu s + A_1 \partial_\mu B_1 + A_2 \partial_\mu B_2)], \quad (7)$$

with  $n = \sqrt{-J^\mu J^\mu g_{\mu\nu}}$ , and 4-velocity  $u^\alpha = J^\alpha/n$ . We consider several copies of the previous action each describing a different fluid, labeled with an index  $I$ . Then we can expand the previous SSL up to second order in the perturbation fields, and to this one, we then add a correction aimed to describe an anisotropic fluid as follows  $S_m^{(2)} = S_{\text{SSL}}^{(2)} + S_{\text{corr}}^{(2)}$ , where  $S_{\text{corr}}^{(2)} = \int dt d^3x N a^3 \sum_I \sigma_I \Theta_I$  and  $\Theta_I$  stands for a linear combination of perturbation fields. Since for each matter species  $\rho_I = \rho_I(n_I)$ , and  $n_I = \sqrt{-J_I^\mu J_I^\nu g_{\mu\nu}}$ , one can find a relation among  $\delta\rho_I$  and the other fields as  $\delta J_I = \frac{\rho_I}{n_I \rho_{I,n}} \frac{\delta\rho_I}{\rho_I} - \alpha$ , where  $\delta N = N(t)\alpha$ , which can be used as a field redefinition to replace  $\delta J_I$  in terms of  $\frac{\delta\rho_I}{\rho_I}$ . We also define gauge invariant combinations  $v_I = -\frac{a}{k^2} \theta_I + \chi - \frac{a^2}{N} \partial_t(E/a^2)$ ,  $\alpha = \Psi - \frac{\dot{\chi}}{N} + N^{-1} \partial_t[a^2 N^{-1} \partial_t(E/a^2)]$ ,

and  $\zeta = -\Phi - H \chi + \frac{a^2 H}{N} \partial_t(E/a^2)$ , where  $\delta\gamma_{ij} = 2[a^2 \zeta \delta_{ij} + \partial_i \partial_j E]$ , and  $\delta u_{Ii} = \partial_i v_I$ . We find finally that

$$S_{\text{corr}}^{(2)} = \int dt d^3x N a^3 \sum_I \sigma_I [\delta\rho_I + 3(\rho_I + P_I) \zeta]. \quad (8)$$

For vector transverse modes, we can define  $T_{Ij}^i \equiv p_I \delta^i_j + p_I \frac{\delta^{ik}}{a^2} \pi_{kj}^I$ , and  $\pi_{ij}^I \equiv \frac{1}{2} (\partial_i \pi_j^{I,T} + \partial_j \pi_i^{I,T})$ . Then we can introduce the 1+3 decompositions for the 4-velocity of the fluid  $u_{Ii}^{V,I} = \delta u_{Ii}^I$ , the shift  $N_i = a N G_i$ , and the 3D metric  $\delta\gamma_{ij} = a(\partial_i C_j + \partial_j C_i)$ . We can also introduce the following gauge invariant variables  $V_i = G_i - \frac{a}{N} \frac{d}{dt} \left( \frac{C_i}{a} \right)$ , and  $F_i^I = \frac{C_i}{a} - \frac{b_{1i}^I}{b_1^I \cdot b_1^I} \delta B_1^I - \frac{b_{2i}^I}{b_2^I \cdot b_2^I} \delta B_2^I$ , where  $b_{1i}^I b_{2i}^I = 0 = b_{1i}^I k^i = b_{2i}^I k^i$ . Then, on following a similar approach one finds the total Lagrangian density for the vector perturbations, in  $\Lambda$ CDM, can be written as

$$\begin{aligned} \mathcal{L} = N a^3 \delta^{ij} \left\{ \sum_I n_I \rho_{I,n} \frac{\dot{F}_i^I}{N} \delta u_j^I + \frac{1}{a^2} \sum_I n_I \rho_{I,n} \left[ a \delta u_i^I V_j - \frac{1}{2} \delta u_i^I \delta u_j^I \right] - \frac{M_P^2}{4a^2} V_i (\delta^{lm} \partial_l \partial_m V_j) \right. \\ \left. - \frac{1}{2a^2} \sum_I p_I \pi_i^{I,T} (\delta^{lm} \partial_l \partial_m F_j^I) \right\}, \end{aligned} \quad (9)$$

which reduces to the same result as in GR.

Finally, for the tensor modes, let us define  $\delta\gamma_{ij} = a^2 (h_+ \varepsilon_{ij}^+ + h_\times \varepsilon_{ij}^\times)$ , where  $\varepsilon_{ij}^{+, \times} = \varepsilon_{ji}^{+, \times}$ ,  $\delta^{ij} \varepsilon_{ij}^{+, \times} = 0$ ,  $\varepsilon_{ij}^+ \varepsilon_{mn}^\times \delta^{im} \delta^{jn} = 0$ , and  $\varepsilon_{ij}^+ \varepsilon_{mn}^+ \delta^{im} \delta^{jn} = 1 =$

$\varepsilon_{ij}^\times \varepsilon_{mn}^\times \delta^{im} \delta^{jn}$ . As for the energy-momentum tensor we have instead for the perturbations  $\delta T_{ij}^i \equiv p_I \frac{\delta^{ik}}{a^2} \pi_{kj}^{I,TT}$ , so that the total Lagrangian density in  $\Lambda$ CDM becomes

$$\mathcal{L} = \frac{M_P^2}{8} \frac{a^3}{N} (\dot{h}_+^2 + \dot{h}_\times^2) - \frac{N a M_P^2}{8} [(\partial_i h_+) \delta^{ij} (\partial_j h_+) + (\partial_i h_\times) \delta^{ij} (\partial_j h_\times)] + \frac{N a}{2} \sum_I p_I (h_+ \pi_+^I + h_\times \pi_\times^I), \quad (10)$$

which reduces to the same form of GR.

Before substituting the explicit dependence of  $H$  on the redshift  $z$ , all the equations of motion (including the ones for the matter fields) for the perturbations are, in form, exactly the same as for  $\Lambda$ CDM, except the following one (written in terms of the Newtonian-gauge invariant fields  $\Phi$  and  $\Psi$ ):

$$\ddot{\Phi} + aH\Psi = \frac{3[k^2 - 3a^2(\dot{H}/a)]}{k^2[2k^2/a^2 + 9\sum_j(\varrho_j + p_j)]} \sum_i (\varrho_i + p_i) \theta_i, \quad (11)$$

which is used to find the evolution of the curvature perturbation  $\Phi$ , and where a dot represents a derivative with respect the conformal time. At the level of linear perturbation, the deviation from  $\Lambda$ CDM therefore consists of two parts: the explicit difference seen in (11) and the implicit difference due to different  $H(z)$ .

The parameter estimation is made via Markov Chain Monte Carlo (MCMC) sampling by using Monte Python [21, 22] against the above mentioned data sets. In the MCMC sampling we used very high precision by decreasing the step size for both background and pertur-

Experiments	VCDM	$\Lambda$ CDM	$\Delta\chi^2$
Planck_highl_TTTEEE	2349.09	2373.83	24.74
Planck_lowl_EE	396.01	398.94	2.93
Planck_lowl_TT	22.29	20.96	-1.33
Pantheon	1036.43	1036.12	-0.31
bao_boss_dr12	9.04	16.70	7.66
bao_smallz_2014	7.15	6.88	-0.27
Total	3820.02	3853.43	33.41

Table I: Comparison of effective  $\chi^2$  between VCDM and  $\Lambda$ CDM for individual data sets.

bation integration to see the smooth transition of  $H(z)$ . The analysis of the MCMC chains is performed using a chain analyzer package, GetDist [23].

We have considered the prior for the parameters of VCDM such that  $\Lambda$ CDM is well inside the region. In particular, we give  $0.6 < \beta_H < 2.3$ , and  $-0.5 < A_2 < 3$ , fixing  $A_3 = 10^{-3}$  as it has large degeneracy. Deviations of  $\beta_H$  from 1 imply that the cosmological data sets prefer the VCDM model over  $\Lambda$ CDM.

By doing the chain analysis we found a remarkable improvement in the fitness parameter with respect to that of  $\Lambda$ CDM,  $\Delta\chi^2 = 33.41$ . In order to have a better picture of the  $\chi^2$  for cosmological data sets we have considered, in Table I we compare effective  $\chi^2$  of each experiment between VCDM and  $\Lambda$ CDM and also the residue  $\Delta\chi^2$ . The fitness parameter for Planck high- $\ell$  is improved which is in agreement with the studies presented in [24]. In fact, the reduction of the tension presented in this paper relies on this better fit for Planck data given a late time modification of  $H(z)$ , whereas the fit to the Pantheon data is essentially unchanged compared to  $\Lambda$ CDM. Furthermore, through the bestfit value of the parameter  $A_2 \simeq 0.35$  ( $A_2$  fixes the redshift of the transition to a larger  $H$ ), the VCDM theory combined with the cosmological data sets automatically avoids the potential problem of a transition around  $z = 0$  as explained in [16].

Fig. 1 shows 2-dimensional marginalised likelihoods for the cosmological parameters of interest in VCDM model as well as for  $\Lambda$ CDM. The Table II gives the values of the parameters within  $2\sigma$ 's. It is clear that the parameter  $A_2$  has a sharp upper cut off. This can be understood by the following logic. Both BAO and Planck data have a better fit for a dynamics for  $H(z)$  which leads to lower values of  $H_0$  (compared to local measurements in  $\Lambda$ CDM). This behavior still holds for VCDM. This is the reason why not only Planck but also BAO-dr12 data are fit better in VCDM. But for lower redshifts (outside the range of BAO-dr12, for which  $0.38 < z < 0.61$ ), Pantheon data require larger values for  $H(z)$ , and the transition occurs. In order to take into account lower redshift BAO data, we have also considered small- $z$  BAO data (refer to table I). This explains the redshift of transition (related to the  $A_2$  parameter), and probably some similar behavior will be

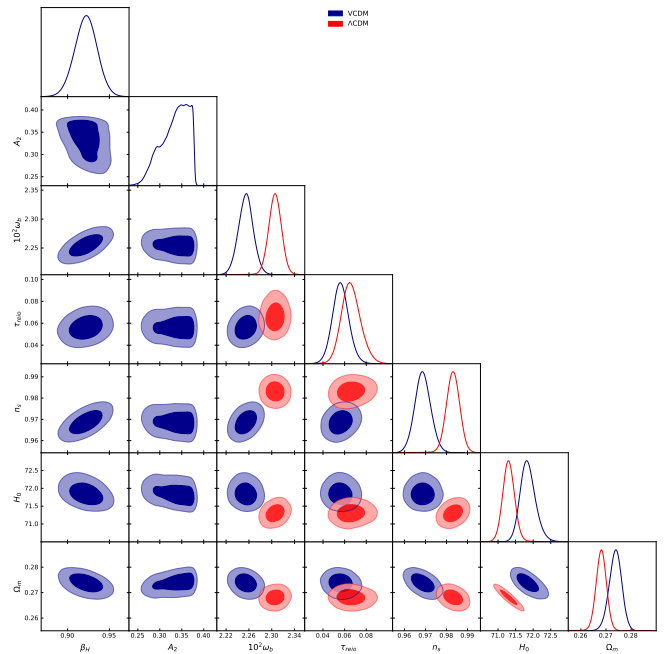


Figure 1: 2-dimensional marginalised likelihoods for the VCDM and  $\Lambda$ CDM model fitting against the cosmological data sets.

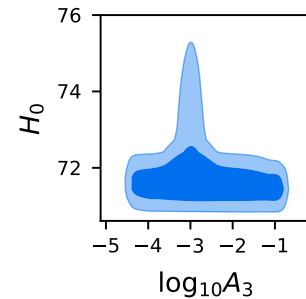


Figure 2: Degeneracy over the parameter  $A_3$ .

required if both current and future cosmological data will keep constraining the  $\Lambda$ CDM profile for  $H(z)$ . As for the width of the transition (related to the  $A_3$  parameter, we have fixed it to the value of  $10^{-3}$ . This does not lead to a fine-tuning: it is just a choice. In fact, if we perform a Montecarlo sampling by adding this third parameter, we find for the same wanted value of  $H_0$  a large degeneracy (about three orders of magnitude at  $1\sigma$ ) for  $A_3$  (see Fig. 2). This only shows that the data are still not powerful enough to give some insight into this parameter. For this reason, we have fixed  $A_3$  to a reasonable value.

From Table II, it is interesting to notice that the value of  $\beta_H$  does not reach 1 even at  $2\sigma$ . It means that the data prefer VCDM over  $\Lambda$ CDM. We find that the bestfit value of Hubble expansion rate today is  $H_0 = 71.73$ , which indicates that the tension is reduced. However we need

	VCDM	$\Lambda$ CDM
Parameters	95% limits	95% limits
$\beta_H$	$0.921^{+0.027}_{-0.026}$	—
$A_2$	$0.355^{+0.025}_{-0.078}$	—
$10^2 \omega_b$	$2.255^{+0.026}_{-0.026}$	$2.304^{+0.024}_{-0.021}$
$\tau_{\text{reio}}$	$0.055^{+0.016}_{-0.014}$	$0.063^{+0.022}_{-0.014}$
$n_s$	$0.97^{+0.01}_{-0.01}$	$0.9833^{+0.006}_{-0.007}$
$10^9 A_s$	$2.097^{+0.073}_{-0.061}$	$2.113^{+0.091}_{-0.064}$
$H_0$	$71.73^{+0.58}_{-0.29}$	$71.22^{+0.46}_{-0.25}$
$\Omega_m$	$0.2748^{+0.0037}_{-0.0062}$	$0.269^{+0.003}_{-0.005}$

Table II: One-dimensional  $2\sigma$  constraints for the cosmological parameters of interest after the estimation with the cosmological data sets considered.

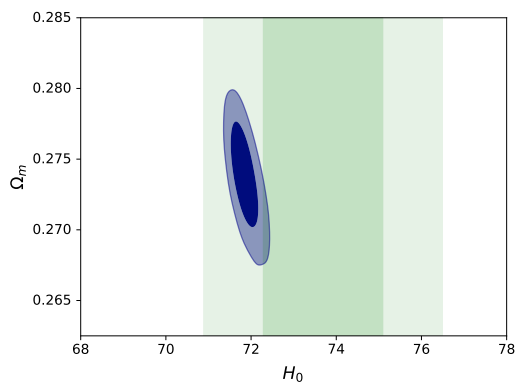


Figure 3:  $\Omega_m - H_0$  contour showing the  $H_0$ -tension is reduced compared with the local determination of  $H_0^{\text{loc}}$  within the VCDM theory. The green shade is  $H_0^{\text{loc}}$ .

to determine the local value of the Hubble expansion rate today  $H_0^{\text{loc}}$  following the analysis explained in [15, 16] (refer to Appendix A for details). We find that the local value of the Hubble expansion today is  $H_0^{\text{loc}} = 73.69 \pm 1.4$ . Fig. 3 shows the contour of  $\Omega_m$  and  $H_0$  determined by the MCMC analysis and also the  $H_0^{\text{loc}}$  with  $2\sigma$  error bars. The tension might be further reduced by introducing the latest analysis presented in [25], where they have reached 1.8% precision by improving the calibration. They find the Hubble expansion today as  $H_0 = 73.0 \pm 1.3$ .

Let us look at the evolution of the background and perturbation variables to see the behaviour of the minimum of VCDM. The behavior of  $H(z)$  in VCDM, with a very small transition in the relatively low redshift region which is visible in Fig. 4, between the redshift 0.3 and 0.4. As explained earlier, an intuitive picture from equation (6) gives the parameter  $\beta_H$  as the amplitude of the transition,  $A_2$  the location of the redshift  $z$  at which the transition happens and  $A_3$  is the width of such transition. It is clear from the choice of  $H(z)$  that this is a low-redshift resolution for Hubble tension. Similar pro-

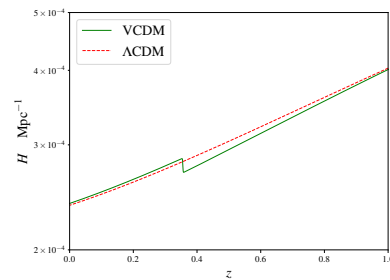


Figure 4: Zoomed version of  $H$  vs  $z$  plot. Here we can see the transition in the  $H(z)$  at very low redshift between 0.3 and 0.4.

posals have been made in [26–30].

In this report we showed that the notorious  $H_0$  tension can be addressed by a very minimal modification to the standard cosmological model, dubbed VCDM. We see that the value of  $H_0^{\text{loc}}$  estimated with this theory reduces the  $H_0$  tension. It is also noticed that this model fits the cosmological data sets better than  $\Lambda$ CDM, mostly Planck high- $\ell$ . The total fitness parameter is improved by 33.41. Background and perturbation variables are stable and finite. Hence we propose the VCDM model as a possible solution to the  $H_0$  tension. We need further investigation to look at whether VCDM can address the tension in the large-scale structure,  $S_8$  along with the  $H_0$  tension, although as already shown in [8], for this theory  $G_{\text{eff}}/G_N = 1$ , at short scales. The behaviour of reducing  $H_0$  tension within this theory sounds promising and it would be interesting to test this behaviour with future cosmology surveys like EUCLID [31] and LSST [32]. Finally we want to stress here that violations of 4D diffeo are only present in the gravity sector at cosmological scales. Since gravity is modified in the IR limit, and because of the absence of any extra gravitational mode other than the standard tensorial gravitons, we expect that graviton loop corrections to be negligible. Therefore matter sector Lagrangians are fully covariant in 4D, up to  $M_{\text{P}}^2$ -suppressed, tiny radiative corrections.

## Appendix A: Calculation of $H_0^{\text{loc}}$

Here we explain how to determine the local value of Hubble expansion rate today for a given theoretical model. We follow the method explained in [15, 16].

The apparent magnitude of a supernovae at a redshift  $z$  is given by

$$m_B^t(z) = 5 \log_{10} \left[ \frac{d_L(z)}{1 \text{ Mpc}} \right] + 25 + M_B, \quad (\text{A1})$$

where  $d_L(z)$  is the luminosity distance and  $M_B$  is the absolute magnitude. The superscript  $t$  in  $m_B^t(z)$  stands for theoretical apparent magnitude. The luminosity distance

is given by

$$d_L = \frac{c}{H_0} (1+z) \int_0^z \frac{dz'}{E(z')}, \quad (\text{A2})$$

where  $E = H/H_0$ . Then the apparent magnitude can be rewritten as

$$m_B^t = 5 \log_{10} \left[ (1+z) \int_0^z \frac{dz'}{E(z')} \right] - 5 \log_{10} \left[ \frac{(1 \text{Mpc}) H_0}{c} \right] + 25 + M_B. \quad (\text{A3})$$

Now we define

$$\begin{aligned} \tilde{m}_B^t &= m_B^t - M_B + 5 \log_{10} \left[ \frac{(1 \text{Mpc}) H_0}{c} \right] \\ &= 5 \log_{10} \left[ (1+z) \int_0^z \frac{dz'}{E(z')} \right] + 25, \end{aligned} \quad (\text{A4})$$

which does not depend on both  $H_0$  and  $M_B$ , but only on the dynamics of  $E(z)$ , which is a function of the other parameters of  $\Lambda$ CDM. We would then introduce the residual

$$m_{B,i} - m_{B,i}^t = m_{B,i} - \tilde{m}_{B,i}^t - M_B + 5 \log_{10} \left[ \frac{(1 \text{Mpc}) H_0}{c} \right],$$

to find a  $\chi^2$  distribution out of it. On calling

$$\begin{aligned} W_i &= m_{B,i} - \tilde{m}_{B,i}^t \\ &= m_{B,i} - \left( 5 \log_{10} \left[ (1+z) \int_0^z \frac{dz'}{E(z')} \right] + 25 \right), \end{aligned} \quad (\text{A5})$$

we then need to find the residues on the variable

$$\begin{aligned} \chi^2 &= (m_{B,i} - m_{B,i}^t) \Sigma_{ij}^{-1} (m_{B,j} - m_{B,j}^t) \\ &= \left( W_i - M_B + 5 \log_{10} \left[ \frac{(1 \text{Mpc}) H_0}{c} \right] \right) \Sigma_{ij}^{-1} \\ &\quad \left( W_j - M_B + 5 \log_{10} \left[ \frac{(1 \text{Mpc}) H_0}{c} \right] \right). \end{aligned} \quad (\text{A6})$$

Now consider

$$\bar{d}_L \equiv (1+z) \int_0^z \frac{dz'}{E(z')}, \quad (\text{A7})$$

so that

$$\bar{d}'_L = \frac{dz}{dN} \frac{\bar{d}_L}{dz} = \bar{d}_L + \frac{(1+z)^2}{E(z)}, \quad (\text{A8})$$

where we have used

$$\frac{dz}{dN} = 1+z, \quad (\text{A9})$$

considering  $N = \ln(a_0/a) = \ln(1+z)$ . Now we can solve for  $\bar{d}_L(z)$ , given the initial conditions  $\bar{d}_L(0) = 0 = z(0)$ .

Once we have the quantities  $\bar{d}_L$  for any data-redshift, we have  $W_i$  so that we are able to find

$$S_0 \equiv V^T \Sigma^{-1} V, \quad (\text{A10})$$

$$S_1 \equiv W^T \Sigma^{-1} V, \quad (\text{A11})$$

where  $V_i = 1$  and  $\Sigma_{ij}$  is the covariance matrix.

Finally, the mean value and the variance of  $H_0^{\text{loc}}$  can be determined by the log-normal distribution

$$H_0^{\text{loc}} = e^{\mu_{\ln} + \frac{1}{2} \sigma_{\ln}^2}, \quad (\text{A12})$$

$$\sigma_{H_0^{\text{loc}}}^2 = \left( e^{\sigma_{\ln}^2} - 1 \right) e^{2\mu_{\ln} + \sigma_{\ln}^2}, \quad (\text{A13})$$

where

$$\mu_{\ln} = \frac{\ln 10}{5} \left[ \bar{M}_B + \frac{\ln 10}{5} \left( \sigma_M^2 + \frac{1}{S_0} \right) - \frac{S_1}{S_0} \right], \quad (\text{A14})$$

$$\sigma_{\ln} = \frac{\ln 10}{5} \sqrt{\sigma_M^2 + \frac{1}{S_0}}, \quad (\text{A15})$$

which, in turn, only depends on  $M_B$ ,  $\sigma_M^2$ ,  $S_0$  and  $S_1$ . Also one should notice that  $S_0$  is only given by the data, and it does not depend on the model, but  $S_1$  does depend on the values of  $\bar{d}_L$ 's, and this will affect  $H_0^{\text{loc}}$  for different models. To get a log-normal distribution we assumed a Gaussian distribution for  $M_B$  and have marginalized over it (refer to [15] for details).

Now we select the the supernovae data and the covariance matrix from Pantheon<sup>2</sup> dataset up to  $z \leq 0.15$ , according to [15]. Then we integrate the luminosity distance with respect to  $N$  to find  $S_1$ . From [15] we use the values  $\bar{M}_B = -19.2322$  and  $\sigma_M = 0.0404$ . Hence we find the values of  $H_0^{\text{loc}}$  and  $\sigma_{H_0^{\text{loc}}}^2$ .

Further study is necessary to understand whether this late time change can fully address today's cosmological puzzles, including the  $S_8$  tension. However, we think this study might help people focusing their efforts on finding the best profile for  $H(z)$  which can model the data sets.

The work of A.D.F. was supported by Japan Society for the Promotion of Science Grants-in-Aid for Scientific Research No. 20K03969. The work of S.M. was supported by JSPS KAKENHI Grant Numbers 17H02890, 17H06359, and by WPI MEXT, Japan. M.C.P. acknowledges the support from the Japanese Government (MEXT) scholarship for Research Student. Numerical computation in this work was carried out at the Yukawa Institute Computer Facility.

---

\* antonio.defelice@yukawa.kyoto-u.ac.jp

† shinji.mukohyama@yukawa.kyoto-u.ac.jp

‡ masroor.cp@yukawa.kyoto-u.ac.jp

[1] Adam G. Riess, Stefano Casertano, Wenlong Yuan, Lucas M. Macri, and Dan Scolnic. Large Magellanic Cloud Cepheid Standards Provide a 1% Foundation for the Determination of the Hubble Constant and Stronger Evidence for Physics beyond  $\Lambda$ CDM. *Astrophys. J.*, 876(1):85, 2019.

<sup>2</sup> <https://github.com/dscolnic/Pantheon>

- [2] Kenneth C. Wong et al. H0LiCOW XIII. A 2.4% measurement of  $H_0$  from lensed quasars:  $5.3\sigma$  tension between early and late-Universe probes. 7 2019.
- [3] M.J. Reid, J.A. Braatz, J.J. Condon, L.J. Greenhill, C. Henkel, and K.Y. Lo. The Megamaser Cosmology Project: I. VLBI observations of UGC 3789. *Astrophys. J.*, 695:287–291, 2009.
- [4] Wendy L. Freedman et al. The Carnegie-Chicago Hubble Program. VIII. An Independent Determination of the Hubble Constant Based on the Tip of the Red Giant Branch. 7 2019.
- [5] N. Aghanim et al. Planck 2018 results. VI. Cosmological parameters. 7 2018.
- [6] Jose Luis Bernal, Licia Verde, and Adam G. Riess. The trouble with  $H_0$ . *JCAP*, 10:019, 2016.
- [7] Adam G. Riess. The Expansion of the Universe is Faster than Expected. *Nature Rev. Phys.*, 2(1):10–12, 2019.
- [8] Antonio De Felice, Andreas Doll, and Shinji Mukohyama. A theory of type-II minimally modified gravity. *JCAP*, 09:034, 4 2020.
- [9] Andrew R Liddle. Information criteria for astrophysical model selection. *Mon. Not. Roy. Astron. Soc.*, 377:L74–L78, 2007.
- [10] N. Aghanim et al. Planck 2018 results. V. CMB power spectra and likelihoods. 2019.
- [11] Florian Beutler, Chris Blake, Matthew Colless, D. Heath Jones, Lister Staveley-Smith, Lachlan Campbell, Quentin Parker, Will Saunders, and Fred Watson. The 6dF Galaxy Survey: Baryon Acoustic Oscillations and the Local Hubble Constant. *Mon. Not. Roy. Astron. Soc.*, 416:3017–3032, 2011.
- [12] Ashley J. Ross, Lado Samushia, Cullan Howlett, Will J. Percival, Angela Burden, and Marc Manera. The clustering of the SDSS DR7 main Galaxy sample – I. A 4 per cent distance measure at  $z = 0.15$ . *Mon. Not. Roy. Astron. Soc.*, 449(1):835–847, 2015.
- [13] Shadab Alam et al. The clustering of galaxies in the completed SDSS-III Baryon Oscillation Spectroscopic Survey: cosmological analysis of the DR12 galaxy sample. *Mon. Not. Roy. Astron. Soc.*, 470(3):2617–2652, 2017.
- [14] D.M. Scolnic et al. The Complete Light-curve Sample of Spectroscopically Confirmed SNe Ia from Pan-STARRS1 and Cosmological Constraints from the Combined Pantheon Sample. *Astrophys. J.*, 859(2):101, 2018.
- [15] David Camarena and Valerio Marra. Local determination of the Hubble constant and the deceleration parameter. *Phys. Rev. Res.*, 2(1):013028, 2020.
- [16] Giampaolo Benevento, Wayne Hu, and Marco Raveri. Can Late Dark Energy Transitions Raise the Hubble constant? *Phys. Rev. D*, 101(10):103517, 2020.
- [17] N. Aghanim et al. Planck intermediate results. LI. Features in the cosmic microwave background temperature power spectrum and shifts in cosmological parameters. *Astron. Astrophys.*, 607:A95, 2017.
- [18] Pavel Motloch and Wayne Hu. Lensinglike tensions in the *Planck* legacy release. *Phys. Rev. D*, 101(8):083515, 2020.
- [19] Diego Blas, Julien Lesgourgues, and Thomas Tram. The Cosmic Linear Anisotropy Solving System (CLASS) II: Approximation schemes. *JCAP*, 1107:034, 2011.
- [20] Masroor C. Pookkillath, Antonio De Felice, and Shinji Mukohyama. Baryon Physics and Tight Coupling Approximation in Boltzmann Codes. *Universe*, 6:6, 2020.
- [21] Benjamin Audren, Julien Lesgourgues, Karim Benabed, and Simon Prunet. Conservative Constraints on Early Cosmology: an illustration of the Monte Python cosmological parameter inference code. *JCAP*, 1302:001, 2013.
- [22] Thejs Brinckmann and Julien Lesgourgues. MontePython 3: boosted MCMC sampler and other features. *Phys. Dark Univ.*, 24:100260, 2019.
- [23] Antony Lewis. GetDist: a Python package for analysing Monte Carlo samples. 10 2019.
- [24] Balakrishna S. Haridasu, Matteo Viel, and Nicola Vittorio. Sources of  $H_0$ -tensions in dark energy scenarios. 12 2020.
- [25] Adam G. Riess, Stefano Casertano, Wenlong Yuan, J. Bradley Bowers, Lucas Macri, Joel C. Zinn, and Dan Scolnic. Cosmic Distances Calibrated to 1% Precision with Gaia EDR3 Parallaxes and Hubble Space Telescope Photometry of 75 Milky Way Cepheids Confirm Tension with LambdaCDM. 12 2020.
- [26] Ryan E. Keeley, Shahab Joudaki, Manoj Kaplinghat, and David Kirkby. Implications of a transition in the dark energy equation of state for the  $H_0$  and  $\sigma_8$  tensions. *JCAP*, 12:035, 2019.
- [27] Kyriakos Vattis, Savvas M. Koushiappas, and Abraham Loeb. Dark matter decaying in the late Universe can relieve the  $H_0$  tension. *Phys. Rev. D*, 99(12):121302, 2019.
- [28] Gongjun Choi, Motoo Suzuki, and Tsutomu T. Yanagida. Quintessence Axion Dark Energy and a Solution to the Hubble Tension. *Phys. Lett. B*, 805:135408, 2020.
- [29] Antonio De Felice, Chao-Qiang Geng, Masroor C. Pookkillath, and Lu Yin. Reducing the  $H_0$  tension with generalized Proca theory. *JCAP*, 08:038, 2020.
- [30] Andrzej Hryczuk and Krzysztof Jodłowski. Self-interacting dark matter from late decays and the  $H_0$  tension. *Phys. Rev. D*, 102(4):043024, 2020.
- [31] Luca Amendola et al. Cosmology and fundamental physics with the Euclid satellite. *Living Rev. Rel.*, 16:6, 2013.
- [32] Alexandra Abate et al. Large Synoptic Survey Telescope: Dark Energy Science Collaboration. 11 2012.